Journal of Power Sources 187 (2009) 581–585

Contents lists available at ScienceDirect

Journal of Power Sources

journal homepage: www.elsevier.com/locate/jpowsour

Short communication

Understanding the characteristics of high-voltage additives in Li-ion batteries: Solvent effects

Young-Kyu Han[a,*], Jaehoon Jung[a], Sunghoon Yu[b], Hochun Lee[c,**]

[a] Corporate R&D, LG Chem, Ltd. Research Park, 104-1, Moonji-dong, Yusung-gu, Daejeon 305-380, Republic of Korea
[b] Battery R&D, LG Chem, Ltd. Research Park, Daejeon 305-380, Republic of Korea
[c] Department of Applied Chemistry, Kumoh National Institute of Technology, Yangho-dong 1, Gumi, Kyeongbuk 730-701, Republic of Korea

ARTICLE INFO

Article history:
Received 25 July 2008
Received in revised form 14 October 2008
Accepted 31 October 2008
Available online 21 November 2008

Keywords:
Lithium-ion battery
Overcharge protection
Electrolyte additive
Density functional theory
Oxidation potential
Ionization potential

ABSTRACT

Calculations are made of the ionization potential (IP) and the oxidation potential (E_{ox}) values of 108 organic molecules that are potential electrolyte additives for the overcharge protection of lithium-ion batteries (LIBs). The calculated E_{ox} values are in close agreement with the experimental ones, where the root-mean-square deviation is 0.08 V and the maximum deviation is 0.15 V. The molecules exhibiting high E_{ox} (>4.5 V) show one of the following two features: (1) IP > 7.70 eV or (2) IP < 7.70 eV with a relatively large molecule size. Consideration of bulk solvent effects, in particular the electrostatic attraction between solute and solvent, is crucial in determining E_{ox}. Considering its accuracy and reliability, the density functional calculation is recommended as a useful tool for screening electrolyte additives for LIBs.

1. Introduction

Overcharge events are an urgent safety issue in the lithium-ion battery (LIB) industry. Presently, electrolyte additives are widely employed for the overcharge protection of commercial-grade LIBs. Among them, a redox shuttle (RS) bypasses the surplus current via a repetitive redox reaction between the cathode and the anode [1–5]. The RS compounds have their own redox potentials, selected to prevent self-discharge or shuttling during charging, which should be 0.3–0.4 V higher than the end-of-charge potential of the cathode. Aromatic compounds are another class of electrolyte additives used for overcharge protection. Polymerizable monomers such as cyclohexyl benzene (CHB) and biphenyl (BP) are electrochemically oxidized at the overcharged cathode to form a passive polymeric film at the cathode|electrolyte interface [6–12]. In addition, non-polymerizable aromatic compounds such as tert-butyl benzene act as redox mediators, which facilitate oxidative decomposition of electrolyte solvents that leads to gas evolution [6].

Regardless of the mechanism of overcharge protection, the electrolyte additives should remain inert during the normal operation of LIBs and become active only at overcharge events; this requires the additives to have an oxidation potential that is 0.3–0.4 V higher than the cathode potential. For instance, $LiCoO_2$ reaches the fully charged state near 4.2 V (vs. Li/Li^+) and therefore requires additives with an oxidation potential higher than 4.5 V. Thus, determination of the oxidation potential is a crucial step in evaluating novel electrolyte additives.

By means of density functional theory calculations, the present work has obtained the oxidation potentials of 108 organic molecules, which are possible candidates for LIB additives. Calculation accuracy is assessed through comparison with experimental data. Understanding the relationship between the oxidation potential and the molecular characteristics is considered to be very useful for developing novel electrolyte additives with specified oxidation potentials.

1.1. Calculation details

Density functional theory (DFT) has become a popular method for calculating oxidation potentials for a vast array of organic molecules used in LIBs [13–16]. The ground-state structures of the molecules have been fully optimized within C_1 symmetry by means of DFT methods. Spin-restricted and unrestricted schemes have been employed for even- and odd-numbered electron systems, respectively. All DFT geometry optimizations were obtained using DMol3 numerical-based density-functional computer

* Corresponding author. Tel.: +82 428662524; fax: +82 428612057.
** Corresponding author.
E-mail addresses: ykhan@lgchem.com (Y.-K. Han), dukelee@kumoh.ac.kr (H. Lee).

0378-7753/$ – see front matter © 2008 Elsevier B.V. All rights reserved.
doi:10.1016/j.jpowsour.2008.10.137

software [17,18] implemented in the Materials Studio Modeling 3.2 package from Accelrys, Inc. The Kohn–Sham equation was calculated with the gradient-corrected BPW91 functional: the 1988 exchange functional of Becke [19] with the correlation functional of Perdew and Wang [20]. A numerical basis set of double-zeta plus polarization (DNP) quality was employed. Utilizing the geometries obtained at the BPW91/DNP level, single-point energy calculations were performed at the B3PW91/6-31 + G(d,p) level of theory. The functional includes a three-parameter adiabatic connection exchange term [21], i.e., a linear combination of exact Hartree–Fock exchange, Slater exchange [22], and B88 gradient-corrected exchange [19].

This study employs the conductor-variant polarized continuum model (CPCM) [23], which places the solute in a molecular-shaped cavity imbedded in a continuum dielectric medium. In the CPCM models, the variation of the free energy when going from vacuum to solution is composed of the work required to build a cavity in the solvent (cavitation energy) together with the electrostatic (solute–solvent interaction and solute polarization) and non-electrostatic work (dispersion and repulsion energy). A dielectric constant of 31.9 is adopted and is a weighted average value between the dielectric constants of ethylene carbonate (EC: 89.2) and ethyl methyl carbonate (EMC: 2.9), because EC/EMC = 1/2 solution is used as the solvent in cyclic voltammetry experiments. The solvation energies obtained from the CPCM calculations are free energies. In the self-energy of the solute, the entropy and zero-point contributions are omitted due to molecular modes, assuming that they would make only a relatively minor contribution to the desired oxidation potentials [24,25]. All of the single-point DFT and CPCM calculations are carried out by using the program package Gaussian03 [26].

Table 1
Solvent effects [ΔG (cation) − ΔG (neutral) in eV] on oxidation potentials for molecules presented in Figs. 1 and 2.

ID	ΔG_{sol}	ΔG_{cav}	ΔG_{elec}	ΔG_{disp}	ΔG_{rep}
1	−1.71	−0.02	−1.69	0.00	0.00
2	−1.69	0.00	−1.69	0.00	0.00
3	−1.97	0.00	−1.97	0.00	0.00
4	−1.65	−0.02	−1.62	−0.01	0.00
5	−1.99	0.00	−1.99	0.00	0.00
6	−1.91	0.00	−1.91	0.00	0.00
7	−1.70	−0.02	−1.68	0.00	0.00
8	−2.23	0.01	−2.24	0.00	0.00
9	−1.79	0.00	−1.79	0.00	0.00
10	−1.94	0.00	−1.94	0.00	0.00
11	−1.65	−0.01	−1.64	0.00	0.00
12	−1.91	0.00	−1.91	0.00	0.00
13	−1.94	−0.04	−1.88	−0.02	0.00
14	−1.93	0.01	−1.94	0.00	0.00
15	−1.90	0.00	−1.90	0.00	0.00
16	−1.87	0.00	−1.87	0.00	0.00
17	−2.03	0.00	−2.03	0.00	0.00
18	−1.67	−0.01	−1.65	−0.01	0.00
19	−1.84	0.00	−1.84	0.00	0.00
20	−2.05	0.00	−2.05	0.00	0.00
21	−1.92	0.00	−1.92	0.00	0.00
22	−1.28	−0.01	−1.26	−0.01	0.00
23	−1.79	0.01	−1.80	0.00	0.00
24	−1.86	0.01	−1.87	0.00	0.00
25	−1.82	0.00	−1.82	0.00	0.00
27	−1.88	0.00	−1.88	0.00	0.00
28	−1.85	0.03	−1.89	0.01	0.00
29	−1.75	0.00	−1.75	0.00	0.00
30	−1.79	0.00	−1.79	0.00	0.00
34	−1.91	−0.01	−1.90	0.00	0.00
35	−1.91	0.01	−1.92	0.00	0.00
41	−1.98	0.00	−1.98	0.00	0.00
61	−2.05	0.00	−2.05	0.00	0.00

2. Experimental details

Battery-grade 1 M $LiPF_6$ in EC/EMC (1/2, v/v) was chosen as the base electrolyte solution. Using the Karl–Fisher titration method, the water content in the electrolytes was determined to be less than 20 ppm. The free-acid content in the electrolytes was less than 50 ppm.

The oxidation potentials of the benzene derivatives were determined by linear sweep voltammetry (LSV). A Pt disc (area = 0.02 cm^2) was used as the working electrode. The reference electrode was Li foil and the counter electrode was Pt wire. The potential was swept from the open-circuit value to 6 V. The oxidation potentials reported in this paper were obtained from the current–potential curve by measuring the intersection between two extrapolated lines of the residual current line and the increasing oxidation current line.

The preparation of electrolytes and all electrochemical experiments was performed in an argon-atmosphere glove box, in which water and oxygen concentrations were maintained below 5 ppm and the temperature was held at 25 ± 2 °C.

3. Results and discussion

The observed oxidation potential (E_{ox}) values, together with the calculated ionization potential (IP) and E_{ox} values, for 108 molecules are listed in Table 1S (see supplementary data). All potentials are reported vs. Li/Li^+. The calculated oxidation potentials are

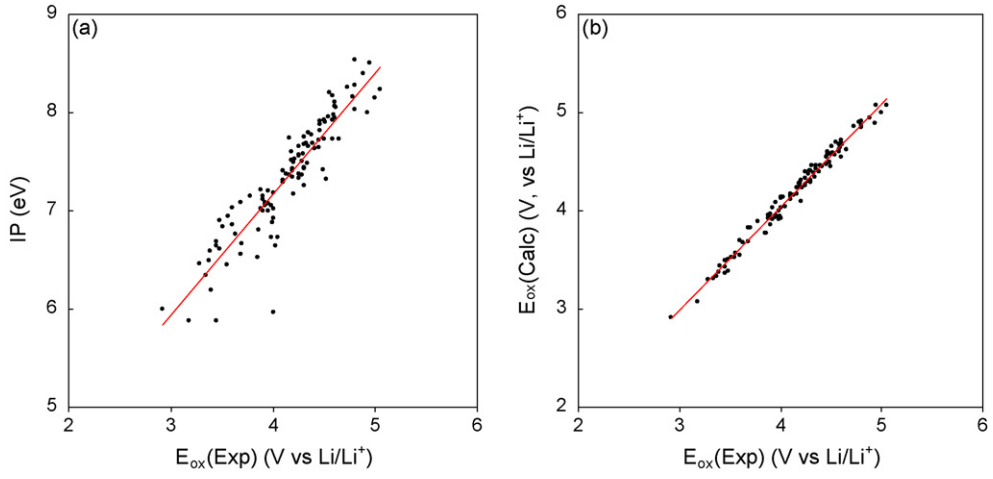

Fig. 1. (a) Ionization potential vs. E_{ox}(exp.); (b) E_{ox}(calc.) vs. E_{ox}(exp.) for all 108 molecules.

in good agreement with the experimental data, where the root-mean-square (RMS) deviation is 0.08 V and the maximum deviation is 0.15 V. The correlation coefficients (R^2) of IP and E_{ox}(calc.) with respect to E_{ox}(exp.) are 0.84 and 0.98, respectively. This observation indicates that consideration of bulk solvent effects is crucial for determining oxidation potentials (see Fig. 1) [27]. The dielectric continuum model, CPCM, provides reliable solvent-driven stabilization effects, in spite of the main limitation of PCM methods, i.e., the total absence of explicit solvent molecules. These results imply that specific short-range interactions are insignificant between ionic solutes and the first-shell of solvent molecules [28]. The observed agreement between the calculated and the experimental oxidation potentials allows estimation of unknown or inaccessible oxidation potentials for organic molecules in such non-aqueous solutions.

Fig. 2 shows 25 high-voltage molecules, each with an E_{ox}(exp.) value greater than 4.50 V. It is worth noting that all the IP values of the molecules are larger than 7.70 eV, except in one case (7.33 eV, molecule **22**). There are only eight molecular groups with the

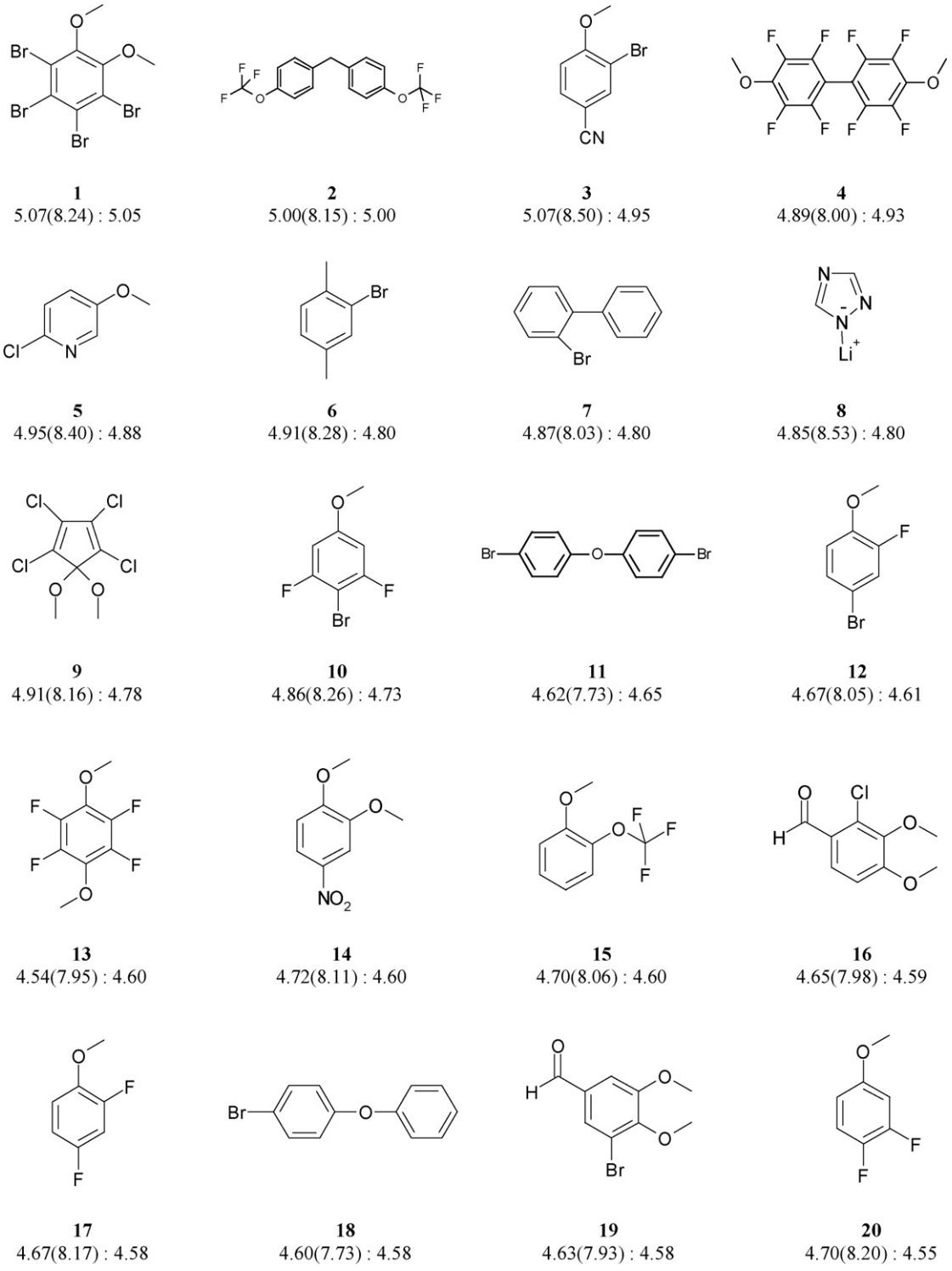

Fig. 2. Twenty-five high-voltage molecules with E_{ox}(exp.) > 4.50 V. E_{ox}(calc.):E_{ox}(exp.) values reported along with IP values in parentheses.

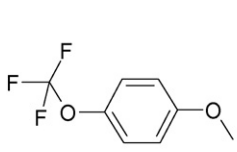

21
4.57(7.96) : 4.54

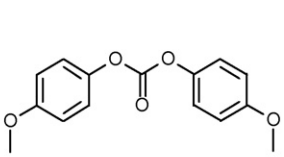

22
4.59(7.33) : 4.52

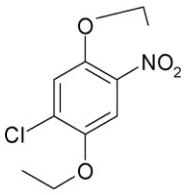

23
4.65(7.90) : 4.51

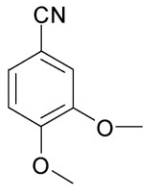

24
4.58(7.93) : 4.50

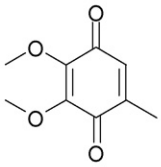

25
4.45(7.73) : 4.50

Fig. 2. (*Continued*).

condition of IP > 7.70 eV and E_{ox} < 4.50 V, as shown in Fig. 3. In the case of molecule **61**, for example, the E_{ox} value is merely 4.16 V, despite having an IP value of 7.74 eV. The solvation energies have been examined in detail to understand such discrepancies between IP and E_{ox} values (see Table 1).

Some remarks need to be made regarding the definition and physical meaning of various solvation energies reported in this study [29,30]. Solvation free energies are calculated as the sum of four different terms, namely: cavitation, electrostatic, dispersion and repulsion energies

$$\Delta G_{sol} = \Delta G_{cav} + \Delta G_{int} = \Delta G_{cav} + \Delta G_{elec} + D_{Gnon\text{-}elec} = \Delta G_{cav} + \Delta G_{elec} + \Delta G_{disp} + \Delta G_{rep} \quad (1)$$

In this expression, ΔG_{cav} is the Gibbs free energy of cavity formation in the liquid solvent; whereas, the following three terms are the electrostatic ΔG_{elec}, dispersion ΔG_{disp}, and repulsion ΔG_{rep} contributions to the energy change ΔG_{int} due to turning on the solute–solvent interactions when the solute is in the cavity. The energy partition scheme employed here can be useful to analyze the nature of the solute–solvent interaction. The solute–solvent electrostatic term is found to be the main interaction between the solute and solvent molecules, as shown in Table 1. The cavitation, dispersion, and repulsion contributions to the oxidation potentials play only a minor role, because such effects for cation and neutral molecules are very similar. It should be noted that the electrostatic interaction energy decreases with increasing molecule size, especially in polar media and when ionic species are involved. Molecule **22** in Fig. 1 has a high voltage of 4.52 V despite having an IP value of 7.33 eV, and has considerably lower absolute solvation energy (−1.28 eV) than the average ΔG_{sol} value of −1.85 eV. The low solvation energy is closely related to the large volume 340.9 Å^3 for molecule **22** with respect to an average value of 212.3 Å^3. For molecule **61** (see Fig. 2), however, the volume 139.9 Å^3 is much

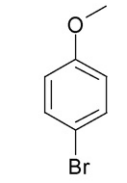

27
4.57(7.91) : 4.46

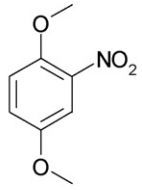

28
4.58(7.88) : 4.46

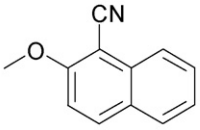

29
4.61(7.82) : 4.46

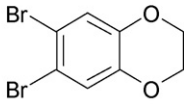

30
4.47(7.72) : 4.45

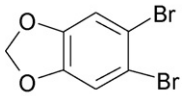

34
4.40(7.77) : 4.38

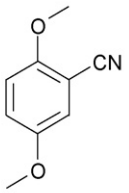

35
4.43(7.80) : 4.35

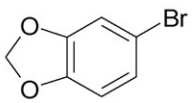

41
4.31(7.76) : 4.30

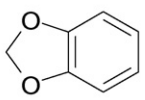

61
4.23(7.74) : 4.16

Fig. 3. Eight molecules with IP > 7.70 eV, E_{ox} < 4.50 V. E_{ox}(calc.):E_{ox}(exp.) values reported along with IP values in parentheses.

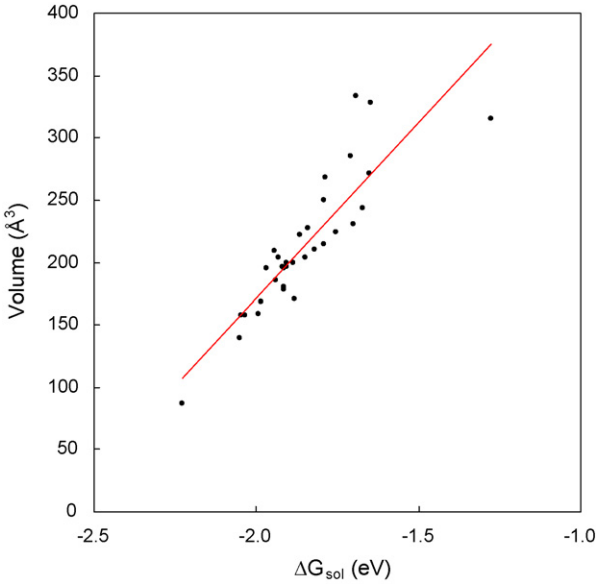

Fig. 4. Molecular volume vs. ΔG_{sol}.

smaller than the average value. Hence, the E_{ox} value is only 4.16 V despite a high IP value of 7.74 eV. The molecular volume and ΔG_{sol} values are plotted in Fig. 4. The correlation coefficient is 0.77, which implies that the oxidation potentials are strongly dependent on the molecular size of the organic molecules commonly used in LIBs.

4. Conclusions

We have calculated their IP and E_{ox} values for comparison purposes with experimental values. The calculated potentials are in close agreement with the experimental values, where the RMS deviation is 0.08 V and the maximum deviation is 0.15 V. Molecules exhibiting high E_{ox} (>4.5 V) show one of the following two features: (1) IP > 7.70 eV or (2) IP < 7.70 eV with a relatively large molecule size. Consideration of bulk solvent effects is important to describe fully the experimental variation in E_{ox}; in particular, the electrostatic attraction between solute and solvent is the most crucial factor. Widely used PCM models reliably estimate the bulk solvent effects for the molecules. Due to its accuracy and reliability, the DFT calculation is recommended for virtual screening of the organic molecules used as electrolyte additives for overcharge protection of LIBs.

Appendix A. Supplementary data

Supplementary data associated with this article can be found, in the online version, at doi:10.1016/j.jpowsour.2008.10.137.

References

[1] J.R. Dahn, J. Jiang, L.M. Moshurchak, M.D. Fleischauer, C. Buhrmester, L.J. Krause, J. Electrochem. Soc. 152 (2005) A1283.
[2] C. Buhrmester, J. Chen, L. Moshurchak, J. Jiang, R.L. Wang, J.R. Dahn, J. Electrochem. Soc. 152 (2005) A2390.
[3] S.S. Zhang, J. Power Sources 162 (2006) 1379, the references are therein.
[4] Z. Chen, K. Amine, Electrochem. Commun. 9 (2007) 703.
[5] L.M. Moshuchak, M. Bulinski, W.M. Lamanna, R.L. Wang, J.R. Dahn, Electrochem. Commun. 9 (2007) 1497.
[6] K. Shima, M. Ue, J. Yamaki, Electrochemistry 71 (2003) 1231.
[7] S. Tobishima, Y. Ogino, Y. Watanabe, J. Appl. Electrochem. 33 (2003) 143.
[8] L. Xiao, X. Ai, Y. Cao, H. Yang, Electrochim. Acta 49 (2004) 4189.
[9] X. Feng, X. Ai, H. Yang, J. Appl. Electrochem. 34 (2004) 1199.
[10] H. Lee, J. Lee, S. Ahn, H.-J. Kim, J.-J. Cho, Electrochem. Solid-State Lett. 9 (2006) A307.
[11] K. Shima, K. Shizuka, M. Ue, H. Ota, T. Hatozaki, J.-I. Yamaki, J. Power Sources 161 (2006) 1264.
[12] H. Lee, S. Kim, J. Jeon, J.-J. Cho, J. Power Sources 173 (2007) 972.
[13] P. Johansson, J. Phys. Chem. A110 (2006) 12077.
[14] C. Buhrmester, L. Moshurchak, R.L. Wang, J.R. Dahn, J. Electrochem. Soc. 153 (2006) A288.
[15] R.L. Wang, C. Buhrmester, J.R. Dahn, J. Electrochem. Soc. 153 (2006) A445.
[16] R.L. Wang, J.R. Dahn, J. Electrochem. Soc. 153 (2006) A1922.
[17] B. Delly, J. Chem. Phys. 92 (1990) 508.
[18] B. Delly, J. Chem. Phys. 113 (2000) 7756.
[19] A.D. Becke, Phys. Rev. A38 (1988) 3098.
[20] J.P. Perdew, Y. Yang, Phys. Rev. B45 (1992) 13244.
[21] A.D. Becke, J. Chem. Phys. 98 (1993) 5648.
[22] S.J. Vosko, L. Wilk, M. Nusair, Can. J. Chem. 58 (1980) 1200.
[23] V. Barone, M. Cossi, J. Tomasi, J. Comput. Chem. 19 (1998) 404.
[24] L.M. Pratt, S. Mogali, K. Glinton, J. Org. Chem. 68 (2003) 6484.
[25] Q. Yang, M.D. Newton, J. Phys. Chem. B112 (2008) 568.
[26] M.J. Frisch, G.W. Trucks, H.B. Schlegel, G.E. Scuseria, M.A. Robb, J.R. Cheeseman, J.A. Montgomery Jr., T. Vreven, K.N. Kudin, J.C. Burant, J.M. Millam, S.S. Iyengar, J. Tomasi, V. Barone, B. Mennucci, M. Cossi, G. Scalmani, N. Rega, G.A. Petersson, H. Nakatsuji, M. Hada, M. Ehara, K. Toyota, R. Fukuda, J. Hasegawa, M. Ishida, T. Nakajima, Y. Honda, O. Kitao, H. Nakai, M. Klene, X. Li, J.E. Knox, H.P. Hratchian, J.B. Cross, C. Adamo, J. Jaramillo, R. Gomperts, R.E. Stratmann, O. Yazyev, A.J. Austin, R. Cammi, C. Pomelli, J.W. Ochterski, P.Y. Ayala, K. Morokuma, G.A. Voth, P. Salvador, J.J. Dannenberg, V.G. Zakrzewski, S. Dapprich, A.D. Daniels, M.C. Strain, O. Farkas, D.K. Malick, A.D. Rabuck, K. Raghavachari, J.B. Foresman, J.V. Ortiz, Q. Cui, A.G. Baboul, S. Clifford, J. Cioslowski, B.B. Stefanov, G. Liu, A. Liashenko, P. Piskorz, I. Komaromi, R.L. Martin, D.J. Fox, T. Keith, M.A. Al-Laham, C.Y. Peng, A. Nanayakkara, M. Challacombe, P.M.W. Gill, B. Johnson, W. Chen, M.W. Wong, C. Gonzalez, J.A. Pople, Gaussian 03, Revision C.02, Gaussian, Inc., Pittsburgh, PA, 2003.
[27] Y.-K. Han, J. Jung, J.-J. Cho, H.-J. Kim, Chem. Phys. Lett. 368 (2003) 601.
[28] E. Buisine, K. de Villiers, T.J. Eagan, C. Biot, J. Am. Chem. Soc. 128 (2006) 12122.
[29] C. Amorilli, B. Mennucci, J. Phys. Chem. B101 (1997) 1051.
[30] E.B. Stukalin, M.V. Korobov, N.V. Avromenko, J. Phys. Chem. B107(2003) 9692.